





8 | Ecology | Research Article

Dominant nitrogen metabolisms of a warm, seasonally anoxic freshwater ecosystem revealed using genome resolved metatranscriptomics

J. M. Fadum, ^{1,2} M. A. Borton, ³ R. A. Daly, ³ K. C. Wrighton, ^{1,3} E. K. Hall ^{1,2}

AUTHOR AFFILIATIONS See affiliation list on p. 15.

ABSTRACT Nitrogen (N) availability is one of the principal drivers of primary productivity across aquatic ecosystems. However, the microbial communities and emergent metabolisms that govern N cycling in tropical lakes are both distinct from and poorly understood relative to those found in temperate lakes. This latitudinal difference is largely due to the warm (>20°C) temperatures of tropical lake anoxic hypolimnions (deepest portion of a stratified water column), which result in unique anaerobic metabolisms operating without the temperature constraints found in lakes at temperate latitudes. As such, tropical hypolimnions provide a platform for exploring microbial membership and functional diversity. To better understand N metabolism in warm anoxic waters, we combined measurements of geochemistry and water column thermophysical structure with genome-resolved metatranscriptomic analyses of the water column microbiome in Lake Yojoa, Honduras. We sampled above and below the oxycline in June 2021, when the water column was stratified, and again at the same depths and locations in January 2022, when the water column was mixed. We identified 335 different lineages and significantly different microbiome membership between seasons and, when stratified, between depths. Notably, nrfA (indicative of dissimilatory nitrate reduction to ammonium) was upregulated relative to other N metabolism genes in the June hypolimnion. This work highlights the taxonomic and functional diversity of microbial communities in warm and anoxic inland waters, providing insight into the contemporary microbial ecology of tropical ecosystems as well as inland waters at higher latitudes as water columns continue to warm in the face of global change.

IMPORTANCE In aquatic ecosystems where primary productivity is limited by nitrogen (N), whether continuously, seasonally, or in concert with additional nutrient limitations, increased inorganic N availability can reshape ecosystem structure and function, potentially resulting in eutrophication and even harmful algal blooms. Whereas microbial metabolic processes such as mineralization and dissimilatory nitrate reduction to ammonium increase inorganic N availability, denitrification removes bioavailable N from the ecosystem. Therefore, understanding these key microbial mechanisms is critical to the sustainable management and environmental stewardship of inland freshwater resources. This study identifies and characterizes these crucial metabolisms in a warm, seasonally anoxic ecosystem. Results are contextualized by an ecological understanding of the study system derived from a multi-year continuous monitoring effort. This unique data set is the first of its kind in this largely understudied ecosystem (tropical lakes) and also provides insight into microbiome function and associated taxa in warm, anoxic freshwaters.

KEYWORDS microbial ecology, biogeochemistry, nitrogen metabolism, denitrification, DNRA, lake, anaerobes, genomics, gene sequencing, taxonomy

Editor Ryan J. Newton, University of Wisconsin-Milwaukee, Milwaukee, Wisconsin, USA

Address correspondence to J. M. Fadum, jfadum@carnegiescience.edu.

The authors declare no conflict of interest.

See the funding table on p. 15.

Received 2 October 2023 Accepted 13 December 2023 Published 23 January 2024

Copyright © 2024 Fadum et al. This is an open-access article distributed under the terms of the Creative Commons Attribution 4.0 International license.

A quatic biogeochemistry is defined by the microbial consortia that inhabit diverse and rapidly changing ecosystems. However, our understanding of microbially driven biogeochemical transformations and associated taxonomies in inland waters is heavily skewed toward temperate ecosystems. Low-latitude aquatic microbiomes are comparatively poorly characterized and understood despite the demonstrable importance of microbial food webs in tropical lakes (1) and the contributions of diverse microbial metabolisms to local and global biogeochemical cycles (2–5). This geographic disparity presents a significant barrier to understanding the ways in which microbial communities shape ecosystem function and is highlighted by the frequency of microbial members with unclassified taxonomies reported in assessments of tropical lake microbial community composition (6). Furthermore, we know that microbial community composition likely differs between temperate and tropical ecosystems, as exemplified by previous comparisons of Lakes Tanganyika and Baikal (7). However, additional work is needed to understand microbial community structure and biogeochemical cycling in smaller tropical lake ecosystems as well.

One important determinant of microbial community composition and biogeochemical cycling is seasonal or permanent anoxia, which occurs in both temperate and tropical lake ecosystems. However, biogeochemical cycling in tropical lakes, which maintain a stratified water column (either permanently or seasonally), may be particularly distinct from that in their temperate counterparts, in part, due to the warm (>20°C) temperatures of their anoxic waters (compared to ~4°C at temperate latitudes) (8). Therefore, while temperature may limit anaerobic metabolisms in high-latitude lakes, this limitation is often alleviated at lower latitudes. Identifying the dominant microbial metabolisms of warm anoxic waters is not only important for understanding contemporary conditions. This work also provides insight into microbially mediated biogeochemistry under future climate scenarios. Though recent work has gained insight into the microbial ecology of permanent anoxic zones in the open ocean (9–12) and in anoxic waters of temperate and arctic lakes (13–15), microbial-mediated biogeochemistry of warm inland waters that sustain anoxia for all, or parts, of the year remains less well described, with some notable exceptions (7, 16).

Understanding the microbial drivers of nitrogen (N) biogeochemistry in aquatic ecosystems is particularly important because reactive N (NH₄⁺ and NO₃⁻) is one of the principal drivers of primary productivity in inland waters. One important source of reactive N to surface waters in seasonally stratified tropical lakes is the hypolimnion (the deepest layer of a stratified water column) due to the accumulation of reactive N during stratification and release of that reactive N to the epilimnion during turnover (17-21). However, the anaerobic metabolisms (and associated taxa) that contribute to this reactive N accumulation are poorly defined. Therefore, to empirically identify which microbial pathways drive N biogeochemistry in warm anoxic water columns and provide a mechanistic explanation of reactive N accumulation in tropical hypolimnions, we provide the first genome-resolved metatranscriptomic analysis of a tropical lake water column under both oxic and anoxic conditions. We hypothesized that, in addition to the mineralization of organic N, dissimilatory nitrate reduction to ammonium (DNRA), may be a unique feature of warm anoxic hypolimnions and an important contributor to the observed accumulation of NH₄⁺ in the anoxic strata of the water column of our study site, Lake Yojoa.

Lake Yojoa (~83 km² surface area, 1.4 km³ volume, and 27.3 m annual average max depth) is located in the center of a ~337 km² mixed land use/landcover watershed in West-Central Honduras (Fig. 1). The lake supports natural fisheries in addition to one large industrial aquaculture operation. The watershed has persistently warm temperatures (annual average air temperatures above 20°C) and receives approximately 2 m of annual precipitation with the warmest months typically corresponding with the monsoon season (June to October). Primary productivity during the mixed water column phase is largely driven by hypolimnetic nutrients which are released to the epilimnion following water column mixing, typically in November (17, 22).

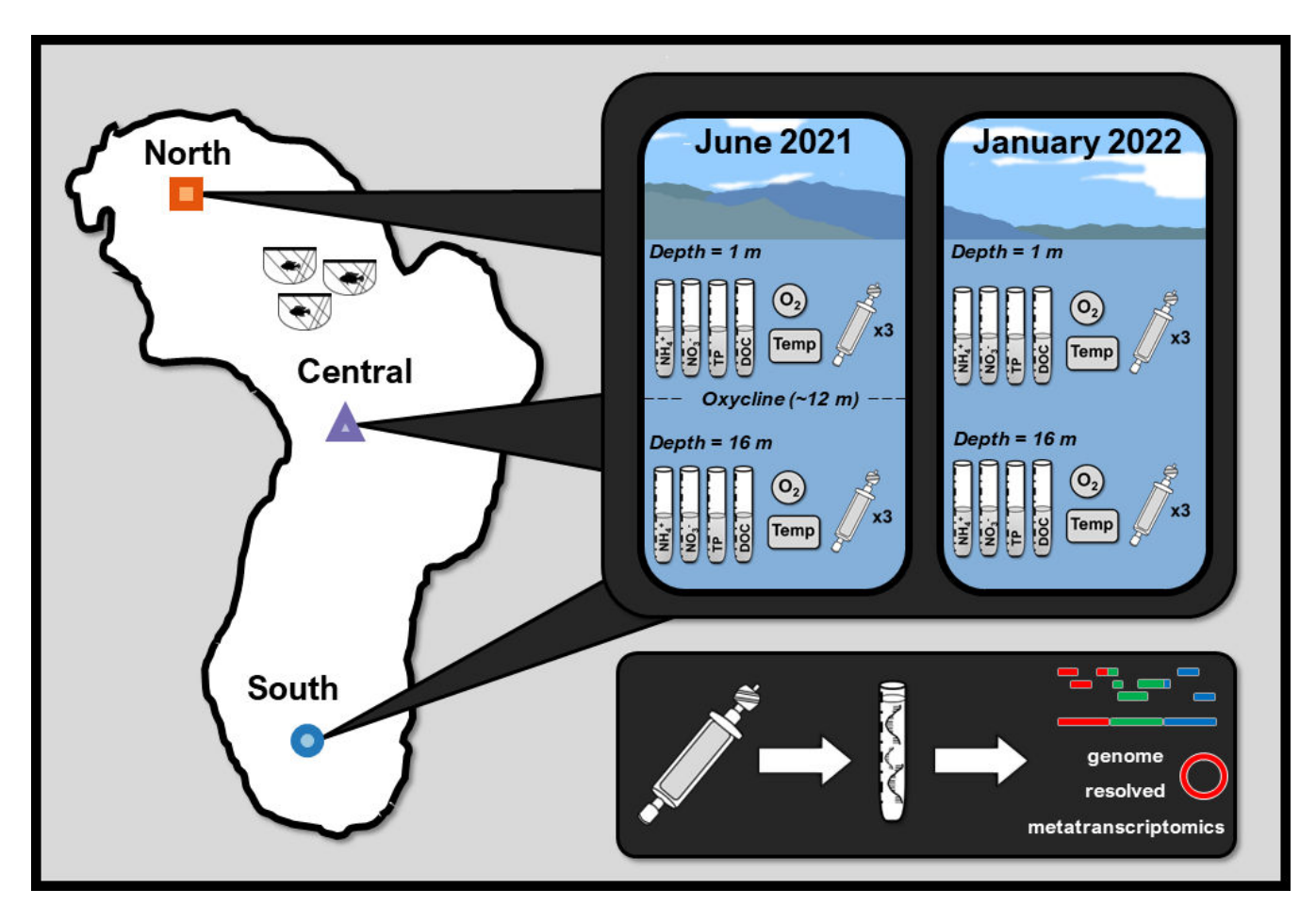


FIG 1 Data collection conceptual figure identifying the three pelagic sampling locations (North, Central, and South) and the types of samples collected (geochemical, thermophysical structure, and metatranscriptome in triplicate) followed by extraction, sequencing, genome assembly, and metatranscriptomic mapping to assembled genome.

RESULTS

Water column redox state and nutrient chemistry

To establish seasonal differences in redox conditions throughout the water column, we compared dissolved oxygen (DO) concentrations in surface and deep waters in June 2021 and again in January 2022. In June, Lake Yojoa was stratified with an oxycline at \sim 12 m depth (which only varied slightly among the three sampling stations; Fig. S1). Therefore, the samples collected in June at 16 m were the only samples taken from an anoxic portion of the water column, while all other samples (June surface and January at both depths) came from oxic waters (Table 1). Although the June hypolimnion was the only reduced environment sample, the temperature was the same as in January across all depths (Table 1). Temperature above 12 m in June significantly (P < 0.001) exceeded temperature in June below the oxycline and at both depths in January.

To assess seasonal and spatial differences in nutrient chemistry, we compared the two dominant forms of reactive N (NH₄ $^+$ and NO₃ $^-$), total phosphorus (TP), and dissolved organic carbon (DOC) between depths and seasons. In January, when the water column was mixed, there was little variation in measured geochemical parameters between the two sampling depths (Fig. 2A through D; Table S1). In contrast, in June, when the water column was stratified, we observed differences in multiple geochemical parameters between the surface and hypolimnion (Fig. 2E through H; Table S1). In particular, hypolimnetic concentrations of NH₄ $^+$ were much greater than surface concentrations of NH₄ $^+$ at all three stations, though differences varied across stations (Fig. 2E). TP was

TABLE 1 Thermophysical structure of Lake Yojoa during sampling events (mean of three sampling locations ± SE)

	June 2021 DO (mgL ⁻¹)	June 2021 Temperature (°C)	January 2022 DO (mgL ⁻¹)	January 2022 Temperature (°C)
	(n =)		(n =)	(n =)
Depth <12 m	6.82 ± 0.23	28.32 ± 0.14	5.51 ± 0.19	24.40 ± 0.02
	(n = 18)	(n = 18)	(n = 18)	(n = 18)
Depth >12 m	0.00 ± 0.00	24.56 ± 0.17	5.14 ± 0.22	24.32 ± 0.02
	(n = 12)	(n = 12)	(n = 12)	(n = 12)

relatively low (<3 μM) across all locations and depths in June and differences between surface (Fig. 2F). Similarly, NO₃ was also low in both the hypolimnion and the surface and not different between strata for all three stations (Fig. 2H). DOC concentrations, though marginally higher in the surface than in the hypolimnion, did not have as pronounced differences as NH_4^+ (Fig. 2G). Geochemical differences in June were primarily characterized by pronounced differences in DO and NH₄⁺ and to a lesser extent TP between strata, whereas geochemistry in January was largely homogeneous between the two depths.

We also identified differences in geochemistry within depths among our three sampling stations. In January, there were few differences among sampling locations at the same depth with the exception of NH₄⁺, which was greater at the northernmost sampling location at both depths (48.00 \pm 0.40 μ M at 1 m and 50.20 \pm 0.10 μ M at 16 m) compared to the central (34.00 \pm 1.01 μM at 1 m and 37.05 \pm 0.95 μM at 16 m) and southern location (32.05 \pm 0.05 μ M at 1 m and 32.35 \pm 0.05 μ M at 16 m; Fig. 2A). In June, hypolimnetic NH₄⁺ was higher at the central station compared to the northern and southernmost stations. Hypolimnetic TP was also greater at the northernmost station (in comparison to the southern and central stations). Surface TP was only noticeably different at the southernmost station. Therefore, while there were quantifiable spatial differences in nutrient chemistry, we did not identify consistent patterns that suggested any particular station was consistently enriched in both reactive N and TP compared to other sampling stations.

Microbiome membership in time and space

Our dereplicated database was composed of 572 metagenomic-assembled genomes (MAGs). However, in order to focus on active biogeochemical pathways, we limited our assessment of microbiome membership to the MAGs detected in the metatranscriptomic data (n = 552). Within the Lake Yojoa metatranscriptome, we identified 335 different lineages (76 classes across 37 phyla). Many genomes represent taxonomies undefined at the family (4.5%), genus (21.1%), or species (86.5%) level. Lineages with novel families often followed unnamed orders (n = 3) or alphanumerically identified orders (n = 13). The abundance of novel lineages in our data set highlights the under-representation of tropical freshwater ecosystems in public genome databases and the degree to which tropical lake microbiomes are still poorly described (6).

The phyla Proteobacteria (n = 97), Bacteroidota (n = 90), Planctomycetota (n = 70), Verrucomicrobiota (n = 66), and Actinobacteriota (n = 56) dominated the represented lineages, as may be expected for freshwater lake ecosystems (23) (Fig. 3A, displayed with Cyanobacteria and Proteobacteria removed). In June 2021, surface waters were dominated with Lyngbya robusta and Microcystis wesenbergii, two common cyanobacteria (24, 25). Cyanobacteria was the most abundant class during both seasons and across both depths. Interestingly, phyla more frequently identified in marine or saline environments, such as Thermoproteota and Halobacteriota, were also identified. Additionally, taxonomies associated with gut microbiomes, including Fibrobacterota, Fusobacteriota, and Firmicutes, were identified. Whereas Firmicutes are ubiquitous in aquatic ecosystems (26), they are also associated with the gut microbiome of Tilapia. This highlights additional

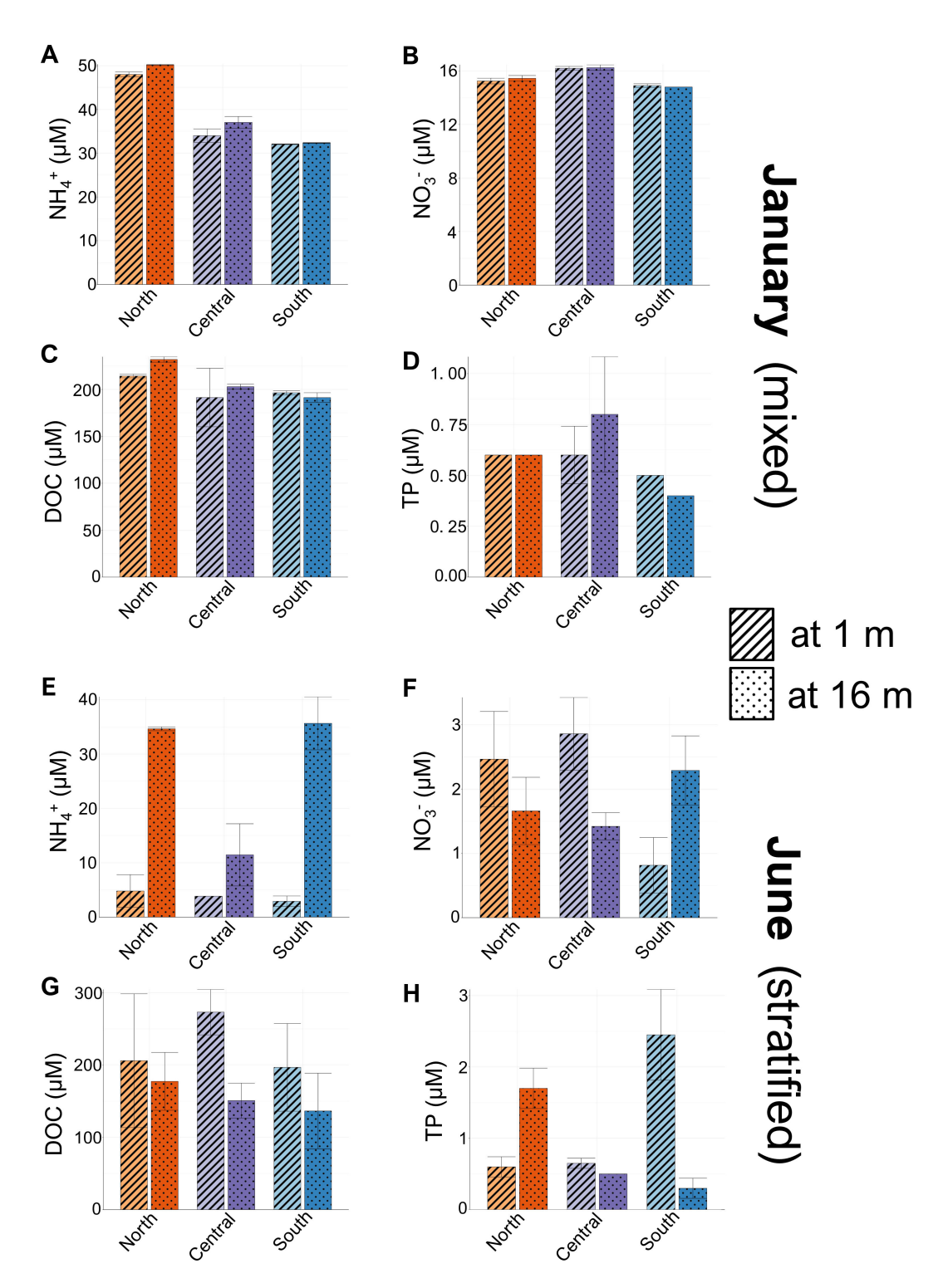


FIG 2 Nutrient concentrations in Lake Yojoa at 1 and 16 m across three sampling locations, mean \pm SE, in January 2022 (A–D) and June 2021 (E–H).

questions regarding the potential impact of Lake Yojoa's industrial aquaculture operation on the lake microbiome (27).

While differences between depths in taxonomy were evident in June at the phyla level (Fig. 3A), differences in taxonomy between the June surface and January (both depths) communities were structured at lower levels of classification (Fig. S2). Given

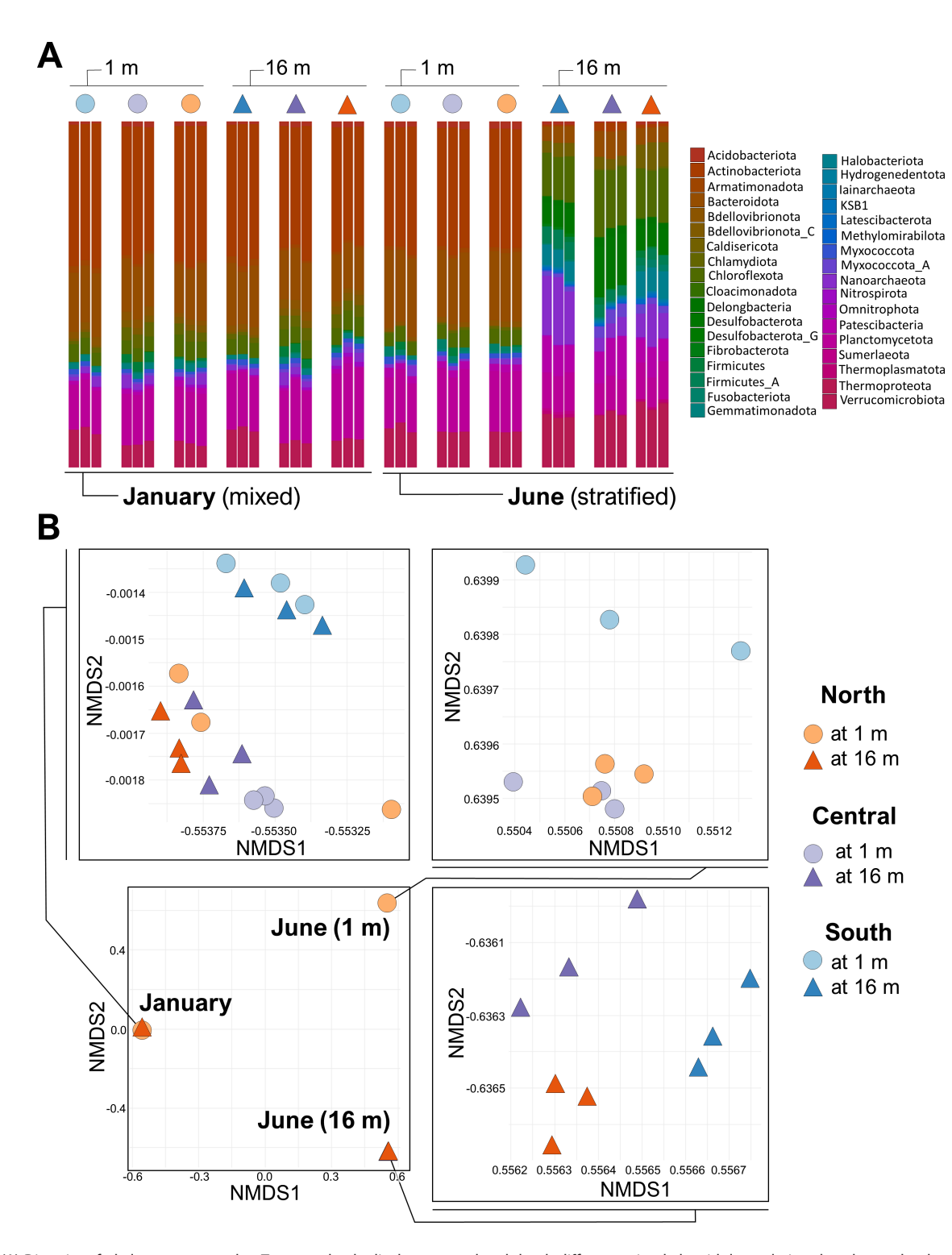


FIG 3 (A) Diversity of phyla among samples. To more clearly display seasonal and depth differences in phyla with low relative abundance, the dominant phyla (*Cyanobacteria* and *Proteobacteria*) were removed from this figure. In January, 28.5% and 28.0% of reads from samples at 1 and 16 m, respectively, were removed. In June, 31.0% and 21.9% of reads from samples at 1 and 16 m, respectively, were removed. Relative abundance was calculated following this removal. (B) Due to highly diverse community assemblages, ordination analysis of MAG expression has been separated into January samples, June surface samples, and June hypolimnetic samples.

the diversity of lineages, we used a nonmetric multidimensional scaling analysis of MAG relative expression within the transcriptome to qualitatively describe differences

in microbial membership within Lake Yojoa in space and time. Due to the dissimilarity of MAG expression among samples, differentiation among all dates and depths within a single two-dimensional ordination analysis was not possible (Fig. 3B). Therefore, to more clearly describe differences in microbiome composition across seasons and among sampling stations, we performed separate ordination analyses on January (both depths), June (surface), and June (hypolimnion) samples (Fig. 3B). In January, we saw no separation in ordination space by depth, as would be expected when the water column was mixed. However, MAG expression in the southern sampling station (at both depths) differed from the other two sampling locations in January. Similarly, MAG expression in the June surface transcriptome at the southern sampling point was also distinct from the other two locations, which were more similar to each other. In the hypolimnion in June, MAG expression at the three sampling locations was all dissimilar (Fig. 3B), likely reflective of decreased physical mixing in the hypolimnion during stratification and station-specific geochemical differences (Fig. 2).

To specifically address the contributions of the microbiome to N cycling, we also identified the taxa of the MAGs that expressed N-cycling genes of interest (Table S2). In January, all taxa expressing N-cycling genes of interest were present at both depths (Fig. S3). Conversely, in June, lineages with N metabolism genes of interest were much more distinct between depths. Many of the identified N cycling families were present only in the hypolimnion in June, while a smaller proportion was present at both 1 and 16 m (and no lineages appeared only at 1 m; Fig. S3).

Dominant microbial N metabolisms

To characterize the dominant N metabolic pathways in our samples, we calculated the relative expression (i.e., number of transcripts) of genes of interest (Table S2) for each station on each date, at each depth. Relative expression within triplicates (from each station) was then summed across stations and within each date and depth hereafter referred to as treatments (i.e., June at 1 m, June at 16 m, January at 1 m, and January at 16 m, n=9 per treatment). We then compared gene expression across each of the four treatments. This allowed us to infer which genes were upregulated or downregulated for a particular treatment relative to all other treatments.

Consistent with trends in the geochemistry data and microbiome membership, we observed similar gene expression for genes involved in N metabolism in January between depths and across stations and dissimilarities in N metabolism gene expression between depths in June (Fig. 4A). In January, at both 1 and 16 m, respiratory NO₂ reductases (*nirB*, *nirD*, *nrfA*, and *nrfH*), NO-forming NO₂ reductase (*nirK*), and assimilatory NO₃ reductases (*narB*, *nasA*, and *nirA*) were the most highly expressed N metabolism genes. Whereas these three gene groups were similarly expressed at both 1 and 16 m, assimilatory NO₃ reductases were upregulated relative to other NO₃ /NO₂ reduction pathways at 1 m compared to at 16 m (Fig. 4). Despite oxic conditions throughout the water column during the January sampling event, we also observed expression of genes involved in several anaerobic metabolisms in January (Fig. 4D and E), including those associated with denitrification beyond NO formation (nitric oxide reductase, *norB/C*, and nitrous oxide reductase, *nosZ*, which was downregulated relative to proceeding steps in denitrification).

The most pronounced differences we observed in N cycling-associated gene expression occurred between the oxic surface and the anoxic hypolimnion in June (Fig. 4C). In the surface, dominant N metabolisms mirrored those in January at 1 m with assimilatory NO₃⁻ reductases being most highly expressed followed by respiratory NO₂⁻ reductases and NO-forming NO₂⁻ reductase. Also, similar to January, *nosZ*, in the June surface, was downregulated relative to previous steps in denitrification. In the hypolimnion, respiratory NO₂⁻ reductases were overexpressed relative to all other gene categories (Fig. 4). Within the respiratory NO₂⁻ reductases, *nrfA* was the most highly expressed gene followed by *nirB*, *nrfH*, and *nirD*, respectively. Collectively, these genes were the most highly expressed across all treatments and stations but had the largest

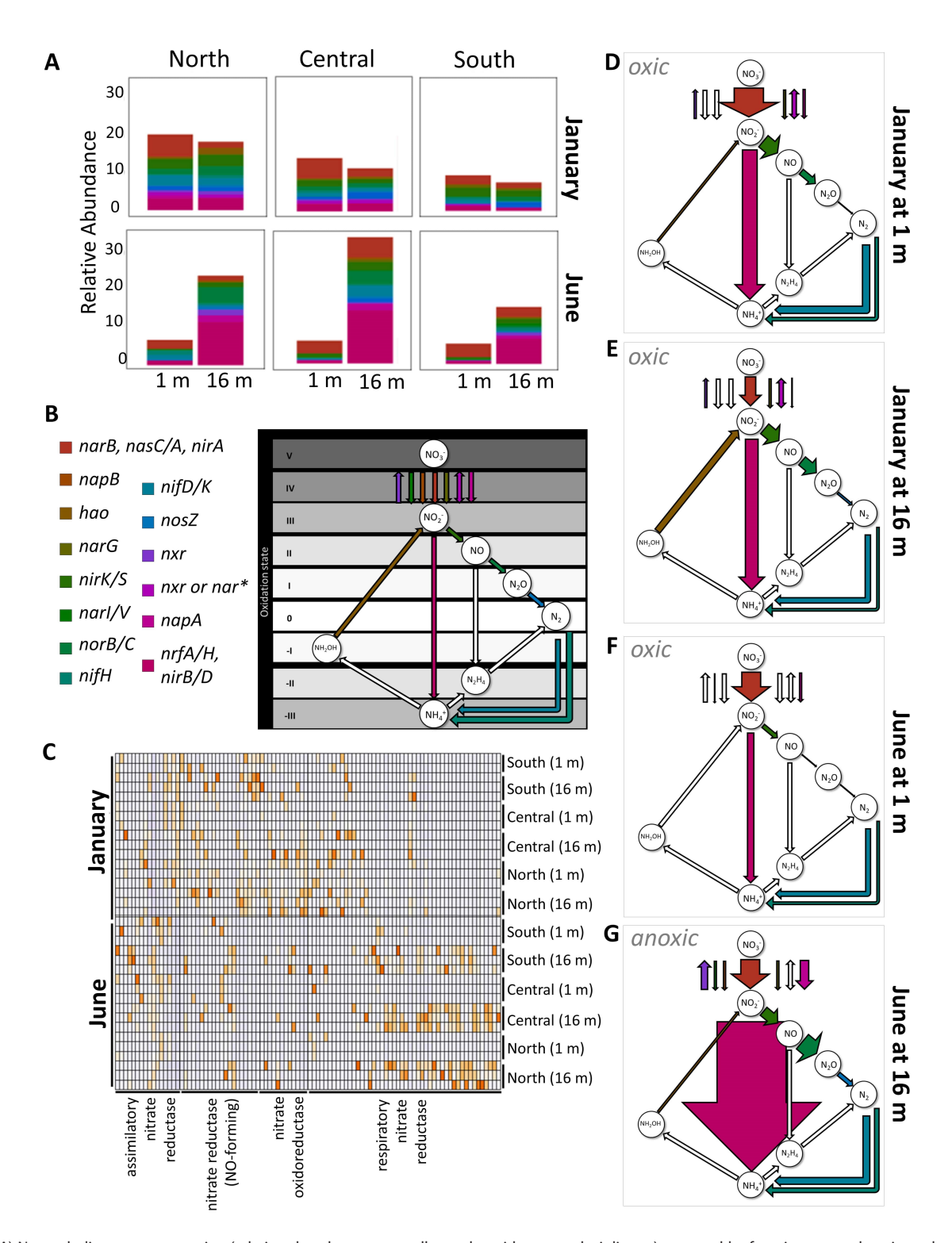


FIG 4 (A) N metabolism gene expression (relative abundance across all samples with summed triplicates), grouped by function, across locations, depths, and season. (B) N cycling pathways assessed in panels D–G, putative transformations. *Differentiation between *nar* and *nxr* expression was not always possible. (C) Heatmap of gene expression of nitrite transformation pathways. (D–G) Conceptual diagram of dominant N transformation pathways across seasons and 1 and 16 m, shown in arrows weighted by expression. Relative abundance data from panel A has been summed by the treatment group. Unfilled arrows represent the complete absence of gene expression.

differential enrichment in the June hypolimnion, indicating strong selection pressure for the pathways these genes are involved in. Using weighted arrows to reflect combined

respiratory nitrate reduction (*nrfA/H* and *nirB/D*), we demonstrate pronounced enrichment of DNRA pathways in June hypolimnion relative to other strata and dates (Fig. 4).

Due to the notable upregulation of respiratory NO₂ reduction genes, we identified the taxa assigned to all genomes that expressed *nirB*, *nirD*, *nrfA*, and *nrfH*. In addition to lineages undefined at the order level, we found 18 orders that were responsible for expressing respiratory NO₂ reductases (Fig. S4). Order *Desulfomonilales* was the most abundant lineage followed by *Anaerolineales*, *Methylococcales*, and an order of *Myxococcota* (*UBA796*). Looking only at lineages expressing *nrfA*, the gene most commonly associated with DNRA (28), 11 of the initially identified 18 lineages (which were performing respiratory NO₂ reduction) were putatively performing DNRA in the hypolimnion (Fig. S5). Lineages from families *Anaerolineaceae*, *Desulfobulbaceae*, and *JAFGLY01* were the most abundant transcribers of *nrfA* with expression being highest in *Anaerolineales Anaerolineaceae*.

Microbial organic N mineralization

To examine additional potential microbial mechanisms that may be responsible for the previously described (17) accumulation of hypolimnetic NH_4^+ , we profiled metatranscriptomic data for expressed peptidases (genes that mineralize organic N into amino acids), organic N transporters (genes for cellular uptake of smaller organic N compounds), amino acid transformers (genes for mineralization of amino acids leading to NH_3^+), and ureases (genes that hydrolyze urea to produce NH_3^+ ; Fig. 5). Collectively, more expression of organic N genes occurred in June relative to January with the most occurring in the hypolimnion, suggesting that mineralization of organic N may also play a role in the previously observed increase in hypolimnetic NH_4^+ during stratification (Fig. 2E) (17).

Categorization of these genes revealed expression in all categories of organic N utilization, including 37,004 peptidases, 5,403 organic N transporters, 214 amino acid transforming genes, and 97 ureases. Genes within the M41 and S14 families had the most expression, with M41 being made up of exopeptidases (cleaves peptide bonds at a terminal end of a protein or peptide) and S14 being made up of endopeptidases (cleaves peptide bonds of non-terminal amino acids). Highly expressed extracellular families included S08A and M23B, made up of endopeptidases that have the potential to cleave after hydrophobic residues and lyse bacterial cell wall peptidoglycans, respectively. Nearly all lineages contributed to peptidase expression, with members of Cyanobacteria, Chloroflexota, and Proteobacteria phyla being the most highly expressed. Similarly, Cyanobacteria and Chloroflexota phyla had the highest average expression within the transporter category. Cyanobacteria also had the most expression in the two most expressed NH₄⁺ forming reactions (urease and aspartate transformations). These results highlight the members of the Cyanobacteria as key contributors to the N cycle in Lake Yojoa, with the highest average expression in all categories of genes involved in organic N cycling.

DISCUSSION

In the Lake Yojoa microbiome, membership and N metabolic gene expression appeared to be primarily influenced by Lake Yojoa's monomictic stratification regime that resulted in pronounced redox differences between water column strata and seasonal depth-specific changes in electron donor and acceptor availability. While there was minimal difference in microbiome membership between depths during January when the water column was mixed, there were distinct differences in membership and gene expression between the surface and the hypolimnion in June. Here, we explore these seasonal and depth discrete differences in Lake Yojoa's microbiome and the role it plays in N cycling by discussing the key results from analyses of the oxic water samples (January at both 1 and 16 m and June at 1 m) within the context of previously observed intra-annual dynamics of the Lake Yojoa ecosystem. We then describe the observed spatial and temporal trends in organic N mineralization across seasons and depths. We conclude the discussion by focusing on the observed NO3⁻ and NO2⁻ reduction pathways we observed in the anoxic

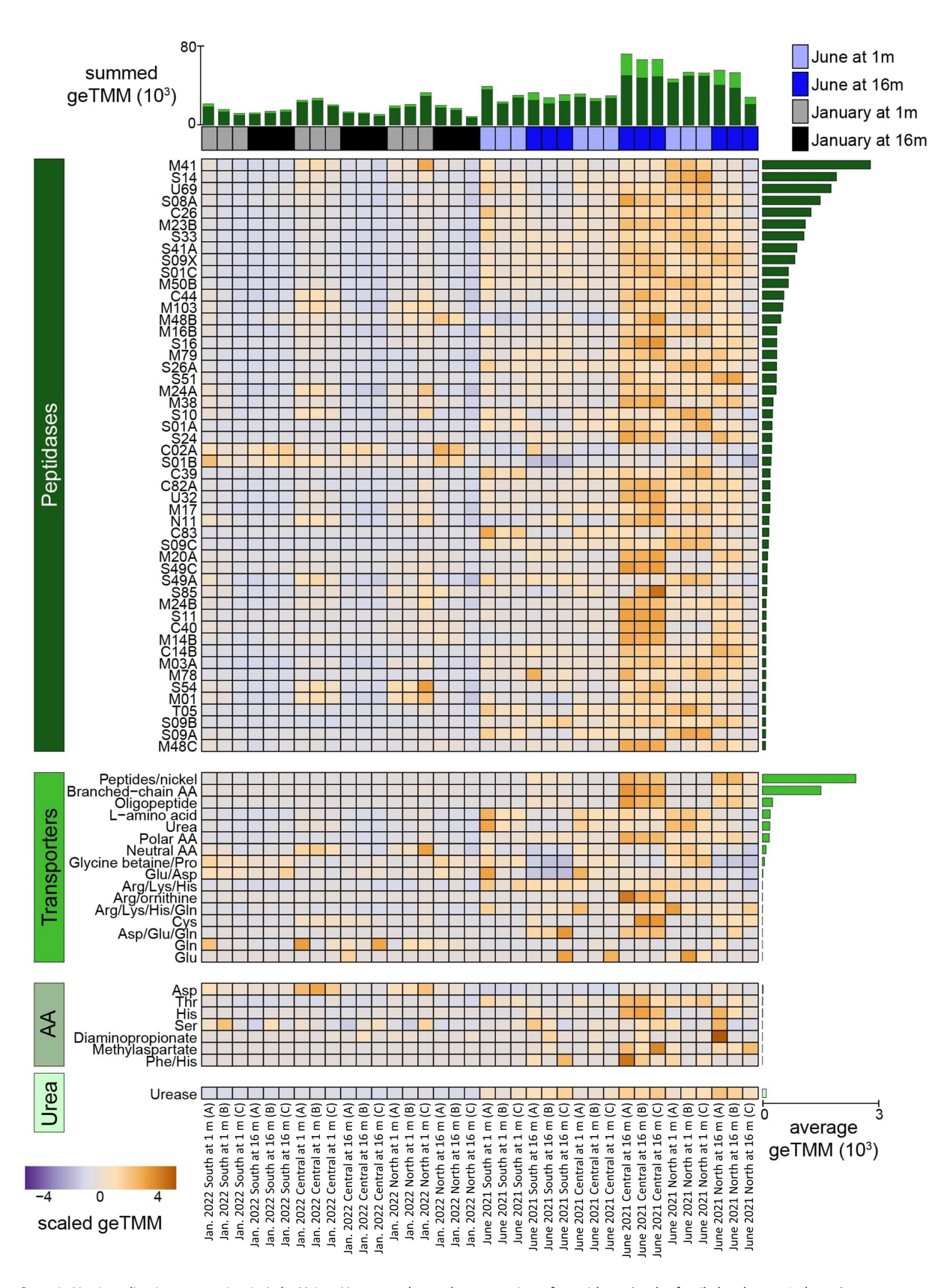


FIG 5 Organic N mineralization expression in Lake Yojoa. Heatmap shows the expression of peptidases (at the family level, top 50 shown), transporters, amino acid transformations, and urease. Expression is scaled within a row and ordered by average transcription across all samples within each category, as depicted by side bar plot. The top stacked bar plot shows the summed expression within each sample, with bars colored by category of organic N shown on the left side of heatmap.

June hypolimnion and characterizing and assessing the putative role of DNRA in NH_4^+ accumulation within Lake Yojoa's warm anoxic hypolimnion.

In June, the downregulation of *napA* (periplasmic nitrate reductase) in the surface (relative to January) was likely due to low concentrations of NO₃, which is depleted in surface waters by June (17). This low abundance of inorganic N in the epilimnion in June relative to January is consistent with previously described N and P colimitation in June but P limitation in January which allows inorganic N to persist at higher concentrations during the mixed water column months (17). As with NO₃, NH₄⁺ was low in the June surface. The absence of *hao* (hydroxylamine oxidoreductase) expression reflects low oxidizable NH₄⁺ availability which would limit nitrification. Conversely, measurable *hao* expression in January was consistent with the increased NH₄⁺ concentration we observed relative to June surface samples. Despite measurable quantities of NH₄⁺ at all sampling points, we were unable to identify the expression of ammonia monooxygenase (*amoA*) for any of the treatments. We assessed our unbinned assembly fractions for *amo*, a function missing in our MAG database. From our assemblies, we recovered a single copy of an *amoA* on a scaffold (<5,000 bp) likely assigned to an unbinned *Nitrosomonas*.

In addition to the expected aerobic metabolisms, we also identified gene expression of putatively anaerobic pathways associated with denitrification and DNRA (e.g., nirK/B, norB/C, nosZ, and nrfA) in the oxic water column. One explanation of this observation is the presence of aerobic denitrifiers (as have been identified in other aquatic ecosystems that experience frequent fluctuation between oxic and anoxic conditions) (29). However, the expression of genes associated with anaerobic metabolisms is more likely explained by the presence of anoxic microsites within the water column (e.g., on sinking particles or other colonized aggregates). Anaerobic metabolisms have been demonstrated to significantly contribute to ecosystem-scale biogeochemical cycling in bulk oxic environments (30), and sinking particulates are hotspots of anaerobic metabolisms in both marine and lake ecosystems (31–33). The presence of anoxic microsites also explains expression within genomes identified as strict anaerobes, such as Desulfomonilia, in the June surface waters and January water column. In Lake Yojoa, sinking particulates (from primary productivity and fish waste associated with aquaculture) provide ample substrate for the formation of anoxic microsites.

The expression of genes related to organic N mineralization pathways was typically higher in June samples compared to January for most peptidases, organic N transporters, amino acid transformers, and ureases. Notable exceptions to this trend include two peptidases, CO2A (cysteine) and SO1B (Serine), and one amino acid transformer (aspartic acid), which were upregulated in January relative to June. For all other peptidases, expression was greatest in June, particularly at 16 m in the central sampling location, nearest to the fish pens (Fig. 1). Mineralization genes were also upregulated at 1 m and, to a lesser extent, 16 m in the northernmost sampling point. These mineralization hotspots likely reflect Lake Yojoa's dominant watershed-derived nutrient sources (three of the six major tributaries are located in the northwest basin of the lake) and industrial aquaculture, also located in the north-central basin (Fig. 1). As dominant wind direction blows north to south, surface particles from the aquaculture operation are transported south to the central location, likely supplying the hypolimnion in mineralizable N-rich organic matter. The outsized role that the aquaculture plays in the nutrient budget of Lake Yojoa suggests that the mineralization of fish waste may be a principal driver and perhaps the most parsimonious explanation for the previously observed accumulation of hypolimnetic NH₄⁺.

In the June hypolimnion, we saw an upregulation in *nrfA* relative to June surface samples. This distinct difference in gene expression between the top and bottom strata mirrors *nrfA* patterns previously reported in Lake Alchichica, Mexico (16), where N-associated gene abundances were also driven by seasonal patterns in stratification. However, gene expression is imperfectly correlated to protein expression (34, 35) and rarely (with some exceptions) correlates with rate processes (36). This limits the biogeochemical inference that can be drawn between the relative abundance of

transcripts and the role of DNRA and other pathways that compete for NO_3^- (e.g., denitrification). Therefore, in the absence of direct rate measurements, we are unable to determine the relative proportion of NO_2^- reduced by DNRA vs denitrification. However, we can conclude that in the June hypolimnion, across all locations, DNRA pathway genes (nrfA/H and nirB/D) were enriched relative to denitrification pathway genes (nirK, nirS, norB, and nosZ), and a principal gene associated with the anammox pathway (hzsA) was absent. Furthermore, nrfA expression was negatively correlated to NO_3^- concentrations in the June hypolimnion ($R^2 = 0.84$). This suggests that DNRA is increasingly competitive under conditions of low NO_3^- availability (37) and is consistent with the observed annual NH_4^+ accumulation that occurs in Lake Yojoa.

The upregulation of *nrfA* for all three stations in Lake Yojoa, which are kilometers apart, differ in maximum depth, and are different distances from large nutrient sources, suggests that DNRA in the hypolimnion of Lake Yojoa is ubiquitous and perhaps a key mechanism for NH₄⁺ accumulation. Further supporting the role of DNRA in Lake Yojoa's N cycle is the presence of several *nrfA* expressing lineages (such as *Anaerolineales*, *Burkholderiales*, and *Desulfobulbales*, Fig. S5) that have been identified as performing DNRA in other ecosystems (38–40). The majority of these lineages were absent in the oxic surface in June, though *nrfA* gene expression in a subset of those orders (i.e., *Burkholderiales*, *Phycisphaerales*, *Tepidisphaerales*, and *UBA1135*) was present at both depths, likely supported by the anoxic microsites discussed above.

Our study highlights the putative contributions of mineralization and DNRA to the hypolimnetic NH₄⁺ pool of a large tropical lake. We acknowledge that multiple other pathways may play an important role in the accumulation of hypolimnetic reactive N (e.g., sediment-derived NH₄⁺ flux [22], mineralization of fish waste, or interactive effects of Lake Yojoa's virome on N cycling [41, 42]). However, DNRA (because of its competition with denitrification) remains a critical pathway for assessing annual N dynamics, particularly in systems, like Lake Yojoa, that experience seasonal N limitation (17). Determining controls on competing NO₃⁻/NO₂⁻ reduction pathways in the warm anoxic waters of Lake Yojoa and other low-latitude lakes is a critical step in broadening our mechanistic understanding of microbially driven biogeochemical processes that influence the trophic state of tropical freshwater ecosystems.

Conclusion

By identifying the dominant N metabolisms that govern intra-annually variable reactive N availability in Lake Yojoa, we provide new insights into the microbial pathways of these understudied warm, seasonally anoxic ecosystems. Descriptions of such pathways may contain clues that distinguish tropical lake biogeochemistry from temperate lake biogeochemistry. Our results highlight the degree to which the largely undescribed taxonomic and functional diversity in such ecosystems define ecosystem-scale nutrient fluxes. We have also demonstrated the need to define controls and constraints on DNRA, in addition to mineralization. By better understanding the microbial assemblages and emergent metabolisms in tropical lakes, particularly in hypolimnions, we may begin to understand how lakes, like Lake Yojoa, as well as lakes at higher latitudes under future climate scenarios, function under contemporary and eminent environmental stressors.

MATERIALS AND METHODS

Field sampling

In June 2021 and January 2022, we collected water for nutrient analyses (NH₄⁺, NO₃⁻, TP, and DOC) from three stations within the lake (Fig. 1) at 1 and 16 m depth using an opaque Van Dorn water sampler. Stations were chosen to be approximately equidistant from each other to capture the potential spatial heterogeneity of the pelagic zone of Lake Yojoa. Methods for sample collection, preservation, transportation, and analysis as

well as thermophysical profile measurements are available in previously published works on Lake Yojoa (17, 22).

For DNA and RNA sample collection, 100-300 mL water samples were concentrated onto $0.22~\mu m$ pore size Sterivex filters (Sigma Aldrich Cat. # SVGP01050) using sterile 60 mL luer-locking syringes. Water was passed through filters until filters were at capacity. Filters were then quickly purged with air to remove excess water, and 3 mL of RNALater (Sigma Aldrich Cat. # R0901500ML) was added. Sealed Sterivex filters were then placed in individual whirl-paks and placed in a cooler.

Although we only compared two sampling dates, the contrast between June 2021, when stratification was fully developed, juxtaposed against January 2022, when the water column was fully mixed, is representative of the geochemical conditions of the two phases of stratification that Lake Yojoa experiences. No disruption to stratification was identified prior to June sampling (22). Thus, the samples taken in June and January are likely representative of the stratified and mixed water column seasons, respectively.

Extraction

Samples for metagenomics were taken during both sampling events (June 2021 and January 2022) from each location (North, Central, and South) and each depth (1 and 16 m) and extracted for DNA (n=12 metagenomes). To maximize genome recovery and build a robust MAG database for metatranscriptome mapping, we performed additional metagenomic sequencing (n=15 metagenomes) on samples collected during 2019 and 2020 sampling campaigns (17, 22). Samples for RNA were paired with the June 2021 and January 2022 metagenomic sampling and collected from the same locations and depths in triplicate (n=36 metatranscriptomes). DNA and RNA were coextracted using ZymoBIOMICS DNA/RNA Miniprep Kit (Zymo Research Cat. # R2002) coupled with RNA Clean and Concentrator-5 (Zymo Research Cat. # R1013). Extracted biomass for DNA ranged from 1.9 to 4.8 ng μ L⁻¹ (3.3 \pm 1.1) in January and 1.1 to 2.1 ng μ L⁻¹ (1.6 \pm 0.3) in June. RNA biomass ranged from 2.0 to 7.6 ng μ L⁻¹ (4.5 \pm 1.6) in January and 1.1 to 5.9 ng μ L⁻¹ (3.2 \pm 1.5) in June. Samples taken at 1 m generally yielded more biomass than those collected at 16 m. Samples were eluted in 40 μ L and stored at -20° C until they were sent for sequencing as described below.

Metagenomic assembly, binning, and annotation

Genomic DNA was prepared for metagenomic sequencing using Plate-based DNA library preparation on the PerkinElmer Sciclone NGS robotic liquid handling system at the Joint Genome Institute. Briefly, 1 ng of DNA was fragmented and adapter ligated using the Nextera XT kit (Illumina) and unique 8 bp dual-index adapters (custom design). The ligated DNA fragments were enriched with 12 cycles of PCR and purified using Coastal Genomics Ranger high throughput agarose gel electrophoresis size selection to 450–600 bp. The prepared libraries were sequenced using an Illumina NovaSeq following a 2 \times 150 nt indexed run recipe.

Resulting fastq files were assembled and binned using the GROWdb pipe-lines (https://github.com/jmikayla1991/Genome-Resolved-Open-Watersheds-database-GROWdb/tree/main/Yojoa_Honduras_Lake). Briefly, three assemblies were performed on each set of fastq files and binned separately: (i) read trimming with sickle (v1.33), assembly with megahit (v1.2.9), and binning with metabat2 (2.12.1); (ii) read trimming with sickle (v1.33), random filtering to 25% of reads, assembly with idba-ud (1.1.0), and binning with metabat2 (2.12.1); (iii) bins derived from the Joint Genome Institute-Integrated Microbial Genomes (JGI-IMG) pipeline were downloaded. All resulting bins were assessed for quality using checkM (v1.1.2), and medium- and high-quality MAGs with >50% completion and <10% contamination were retained.

For paired June 2021 and January 2022 metagenomes, subassemblies were also performed. Specifically trimmed reads from 12 samples were individually mapped to medium- and high-quality MAGs derived from the three assembly types described above using bbmap (perfectmode = t) (43). Unmapped reads for each sample were

then assembled with idba-ud (1.1.0) (44) and binned with metabat2 (2.12.1) (45). These bins were also assessed for quality using checkM (v1.1.2) (46), and MAGs with >50% completion and <10% contamination were retained in the database. The resulting 1,771 MAGs across all samples and assemblies were dereplicated at 99% identity using dRep (v2.6.2) (47) to obtain the dereplicated Yojoa MAG database (n=572 MAGs). MAG taxonomy was assigned using GTDB-tk (v2.0.0) (48) and annotated using Distilled and Refined Annotation of Metabolism (DRAM) (49). Methods for classifying gene homologs were provided in Supplementary Text 1.

Metatranscriptomic mapping and analysis

RNA was prepared for metatranscriptome sequencing according to JGI-established protocols. A summary of JGI's protocols is available in Supplementary Text 2. Resulting fastq files were mapped via Bowtie2 (-D 10 R 2 N 1 L 22 -i S,0,2.50) (50) to the dereplicated Yojoa MAG database (n=572 MAGs). Sam files were transformed to bam files using samtools filtered to 97% id using reformat.sh (51) and name sorted using SAM Tools (28). Reads per gene were then calculated with featureCounts (52). We then performed length normalization, and counts were transformed to geTMM in R using edgeR package (53). The number of reads within "treatment groups" (January at 1 m, January at 16 m, June at 1 m, and June at 16 m) were similar. Reads in June samples were nearly three times as abundant as those in January samples.

Statistical analysis and figure generation

Statistical analyses and figure generation were performed in R (version 4.1.2). Significant differences in geochemical and thermophysical structure data between depths and/or seasons were assessed using a one-way analysis of variance. Circular dendrograms were created using RAWgraphs (54).

ACKNOWLEDGMENTS

Samples were sequenced and processed as a part of the Genome Resolved Open Watersheds (GROW) effort to sequence global watersheds. We thank Tyson Claffey and Richard Wolfe for Colorado State University server management. Additionally, we thank Juan Carlos Sorto for being instrumental in sample collection. The manuscript was improved by feedback from Josué Rodríguez-Ramos. Sample collection was permitted by and lawfully performed in collaboration with the Asociación de Municipios del Lago de Yojoa y su Área de Influencia (AMUPROLAGO) and with additional support by Dr. Erika Tenorio (Zamorano Pan-American Agricultural School, Tegucigalpa, HN).

E.K.H. and J.M.F. were partially supported by NSF DEB # 2120441 during the analysis and preparation of this manuscript. J.M.F. was supported by the Simons Foundation during the final stages of manuscript preparation and submission. M.A.B. and K.C.W. were partially supported by awards from DOE Office of Science, Office of Biological and Environmental Research (BER), grant nos. DE-SC0021350 and DE-SC0023084. A portion of this work was also performed by M.A.B. under a subcontract to K.C.W. from the River Corridor Science Focus Area at Pacific Northwest National Laboratory (PNNL) and funded by the U.S. Department of Energy, Office of Science, Office of Biological and Environmental Research, and Environmental System Science (ESS) Program. PNNL is operated by Battelle Memorial Institute for the U.S. Department of Energy under Contract No. DE-AC05-76RL01830. Metagenomic and metatranscriptomic sequencing was performed at the Joint Genome Institute under a Community Science Program (proposal:10.46936/10.25585/60001289, awarded to K.C.W. and M.A.B.) and the University of Colorado Anschutz's Genomics Shared Resource. Work conducted at JGI (https://ror.org/04xm1d337), a Department of Energy Office of Science User Facility, was supported by the Office of Science of the U.S. Department of Energy operated under Contract No. DE-AC02-05CH11231. Work conducted at the Genomics Shared Resource was supported by the Cancer Center Support Grant (P30CA046934).

AUTHOR AFFILIATIONS

¹Graduate Degree Program in Ecology, Colorado State University, Fort Collins, Colorado, USA

²Department of Ecosystem Science and Sustainability, Colorado State University, Fort Collins, Colorado, USA

³Department of Soil and Crop Sciences, Colorado State University, Fort Collins, Colorado, USA

AUTHOR ORCIDs

J. M. Fadum http://orcid.org/0000-0002-3206-4338

FUNDING

Funder	Grant(s)	Author(s)
National Science Foundation (NSF)	2120441	E. K. Hall
Simons Foundation (SF)	993455	J. M. Fadum
U.S. Department of Energy (DOE)	DE-SC0021350, DE-SC0023084	M. A. Borton
		K. C. Wrighton

AUTHOR CONTRIBUTIONS

J. M. Fadum, Conceptualization, Formal analysis, Investigation, Validation, Visualization, Writing – original draft, Writing – review and editing | M. A. Borton, Data curation, Formal analysis, Funding acquisition, Methodology, Validation, Visualization, Writing – original draft, Writing – review and editing | R. A. Daly, Investigation, Methodology, Writing – review and editing | K. C. Wrighton, Funding acquisition, Methodology, Project administration, Writing – review and editing | E. K. Hall, Conceptualization, Funding acquisition, Investigation, Project administration, Supervision, Writing – review and editing

DATA AVAILABILITY

Raw reads and metagenome assembled genomes are publicly available on NCBI under Bioproject PRJNA946291. Dereplicated metagenome assembled genomes are also publicly available on Zenodo along with annotations, quality statistics, mapping tables, and geochemistry and thermophysical profile data.

ADDITIONAL FILES

The following material is available online.

Supplemental Material

Text S1 (mSystems01059-23-s0001.docx). Additional information on methods for classifying homologs in the MAG database.

Text S2 (mSystems01059-23-s0002.docx). Summary of RNA preparation methods. **Supplemental Materials (mSystems01059-23-s0003.pdf).** Tables S1 and S2 and Fig. S1-S5

Table S3 (mSystems01059-23-s0004.pdf). Supplemental MAG information.

REFERENCES

- Sarmento H. 2012. New paradigms in tropical limnology: the importance of the microbial food web. Hydrobiologia 686:1–14. https://doi.org/10. 1007/s10750-012-1011-6
- Tranvik LJ, Downing JA, Cotner JB, Loiselle SA, Striegl RG, Ballatore TJ, Dillon P, Finlay K, Fortino K, Knoll LB, et al. 2009. Lakes and reservoirs as regulators of carbon cycling and climate. Limnol Oceanogr 54:2298– 2314. https://doi.org/10.4319/lo.2009.54.6_part_2.2298
- Bastviken D, Tranvik LJ, Downing JA, Crill PM, Enrich-Prast A. 2011. Freshwater methane emissions offset the continental carbon sink. Science 331:50. https://doi.org/10.1126/science.1196808
- Panneer Selvam B, Natchimuthu S, Arunachalam L, Bastviken D. 2014. Methane and carbon dioxide emissions from inland waters in India – implications for large scale greenhouse gas balances. Glob Chang Biol 20:3397–3407. https://doi.org/10.1111/gcb.12575

- Zheng Y, Wu S, Xiao S, Yu K, Fang X, Xia L, Wang J, Liu S, Freeman C, Zou J. 2022. Global methane and nitrous oxide emissions from inland waters and estuaries. Glob Chang Biol 28:4713–4725. https://doi.org/10.1111/ gcb.16233
- Aguilar P, Dorador C, Vila I, Sommaruga R. 2018. Bacterioplankton composition in tropical high-elevation lakes of the Andean plateau. FEMS Microbiol Ecol 94:fiy004. https://doi.org/10.1093/femsec/fiy004
- Tran PQ, Bachand SC, McIntyre PB, Kraemer BM, Vadeboncoeur Y, Kimirei IA, Tamatamah R, McMahon KD, Anantharaman K. 2021. Depth-discrete metagenomics reveals the roles of microbes in biogeochemical cycling in the tropical freshwater Lake Tanganyika. ISME J 15:1971–1986. https://doi.org/10.1038/s41396-021-00898-x
- Lewis WM. 1996. Tropical lakes: how latitude makes a difference. Perspect Trop Limnol 4:43–64.
- Ulloa O, Canfield DE, DeLong EF, Letelier RM, Stewart FJ. 2012. Microbial oceanography of anoxic oxygen minimum zones. Proc Natl Acad Sci U S A 109:15996–16003. https://doi.org/10.1073/pnas.1205009109
- Babbin AR, Peters BD, Mordy CW, Widner B, Casciotti KL, Ward BB. 2017.
 Multiple metabolisms constrain the anaerobic nitrite budget in the Eastern tropical South Pacific. Global Biogeochem Cycles 31:258–271. https://doi.org/10.1002/2016GB005407
- Zakem EJ, Mahadevan A, Lauderdale JM, Follows MJ. 2020. Stable aerobic and anaerobic coexistence in anoxic marine zones. ISME J 14:288–301. https://doi.org/10.1038/s41396-019-0523-8
- Zakem EJ, Lauderdale JM, Schlitzer R, Follows MJ. 2021. A flux-based threshold for anaerobic activity in the ocean. Geophys Res Lett 48:e2020GL090423. https://doi.org/10.1029/2020GL090423
- Cabello Yeves PJ, Zemskaya TI, Zakharenko AS, Sakirko MV, Ivanov VG, Ghai R, Rodriguez - Valera F. 2020. Microbiome of the deep Lake Baikal, a unique oxic bathypelagic habitat. Limnol Oceanogr 65:1471–1488. https://doi.org/10.1002/lno.11401
- Cabrol L, Thalasso F, Gandois L, Sepulveda-Jauregui A, Martinez-Cruz K, Teisserenc R, Tananaev N, Tveit A, Svenning MM, Barret M. 2020. Anaerobic oxidation of methane and associated microbiome in anoxic water of Northwestern Siberian lakes. Sci Total Environ 736:139588. https://doi.org/10.1016/j.scitotenv.2020.139588
- Vigneron A, Cruaud P, Culley Al, Couture RM, Lovejoy C, Vincent WF. 2021. Genomic evidence for sulfur intermediates as new biogeochemical hubs in a model aquatic microbial ecosystem. Microbiome 9:46. https://doi.org/10.1186/s40168-021-00999-x
- Pajares S, Merino Ibarra M, Macek M, Alcocer J. 2017. Vertical and seasonal distribution of picoplankton and functional nitrogen genes in a high-altitude warm-monomictic tropical Lake. Freshw Biol 62:1180– 1193. https://doi.org/10.1111/fwb.12935
- Fadum JM, Hall EK. 2022. The interaction of physical structure and nutrient loading drives ecosystem change in a large tropical lake over 40 years. Sci Total Environ 830:154454. https://doi.org/10.1016/j.scitotenv. 2022.154454
- Vincent WF, Wurtsbaugh W, Vincent CL, Richerson PJ. 1984. Seasonal dynamics of nutrient limitation in a tropical high-altitude lake (Lake Titicaca, Peru-Bolivia): application of physiological bioassays. Limnol Oceanogr 29:540–552. https://doi.org/10.4319/lo.1984.29.3.0540
- Wurtsbaugh WA, Vincentr WF, Tapia RA, Vincent CL, Richerson PJ. 1985.
 Nutrient limitation of algal growth and nitrogen fixation in a tropical Alpine lake, Lake Titicaca (Peru/Bolivia). Freshw Biol 15:185–195. https://doi.org/10.1111/j.1365-2427.1985.tb00191.x
- Merino-Ibarra M, Monroy-Ríos E, Vilaclara G, Castillo FS, Gallegos ME, Ramírez-Zierold J. 2008. Physical and chemical limnology of a windswept tropical highland reservoir. Aquat Ecol 42:335–345. https://doi. org/10.1007/s10452-007-9111-5
- Yaseen T, Bhat SU. 2021. Assessing the nutrient dynamics in a Himalayan Warm Monomictic Lake. Water Air Soil Pollut 232:111. https://doi.org/10. 1007/s11270-021-05054-x
- Fadum JM, Waters MN, Hall EK. 2023. Trophic state resilience to hurricane disturbance of Lake Yojoa, Honduras. Sci Rep 13:5681. https://doi.org/10.1038/s41598-023-32712-3
- Newton RJ, Jones SE, Eiler A, McMahon KD, Bertilsson S. 2011. A guide to the natural history of freshwater lake bacteria. Microbiol Mol Biol Rev 75:14–49. https://doi.org/10.1128/MMBR.00028-10

Rejmánková E, Komárek J, Dix M, Komárková J, Girón N. 2011. Cyanobacterial blooms in Lake Atitlan, Guatemala. Limnologica 41:296–302. https://doi.org/10.1016/j.limno.2010.12.003

- Komárek J, Zapomělová E, Šmarda J, Kopecký J, Rejmánková E, Woodhouse J, Neilan BA, Komárková J. 2013. Polyphasic evaluation of Limnoraphis robusta, a water-bloom forming cyanobacterium from Lake Atitlán, Guatemala, with a description of Limnoraphis gen. nov. Fottea 13:39–52. https://doi.org/10.5507/fot.2013.004
- Zhang J, Yang Y, Zhao L, Li Y, Xie S, Liu Y. 2015. Distribution of sediment bacterial and archaeal communities in plateau freshwater lakes. Appl Microbiol Biotechnol 99:3291–3302. https://doi.org/10.1007/s00253-014-6262-x
- Bereded NK, Abebe GB, Fanta SW, Curto M, Waidbacher H, Meimberg H, Domig KJ. 2022. The gut bacterial microbiome of Nile tilapia (*Oreochromis niloticus*) from lakes across an altitudinal gradient. BMC Microbiol. 22:87. https://doi.org/10.1186/s12866-022-02496-z
- Li H, Handsaker B, Wysoker A, Fennell T, Ruan J, Homer N, Marth G, Abecasis G, Durbin R, 1000 Genome Project Data Processing Subgroup. 2009. The sequence alignment/map format and SAMtools. Bioinformatics 25:2078–2079. https://doi.org/10.1093/bioinformatics/btp352
- Marchant HK, Ahmerkamp S, Lavik G, Tegetmeyer HE, Graf J, Klatt JM, Holtappels M, Walpersdorf E, Kuypers MMM. 2017. Denitrifying community in coastal sediments performs aerobic and anaerobic respiration simultaneously. ISME J 11:1799–1812. https://doi.org/10. 1038/ismej.2017.51
- Angle JC, Morin TH, Solden LM, Narrowe AB, Smith GJ, Borton MA, Rey-Sanchez C, Daly RA, Mirfenderesgi G, Hoyt DW, Riley WJ, Miller CS, Bohrer G, Wrighton KC. 2017. Methanogenesis in oxygenated soils is a substantial fraction of wetland methane emissions. Nat Commun 8:1567. https://doi.org/10.1038/s41467-017-01753-4
- Broman E, Zilius M, Samuiloviene A, Vybernaite-Lubiene I, Politi T, Klawonn I, Voss M, Nascimento FJA, Bonaglia S. 2021. Active DNRA and denitrification in oxic hypereutrophic waters. Water Res 194:116954. https://doi.org/10.1016/j.watres.2021.116954
- 32. Capo E, Cosio C, Gascón Díez E, Loizeau J-L, Mendes E, Adatte T, Franzenburg S, Bravo AG. 2023. Anaerobic mercury methylators inhabit sinking particles of oxic water columns. Water Res. 229:119368. https://doi.org/10.1016/j.watres.2022.119368
- Chakraborty S, Andersen KH, Visser AW, Inomura K, Follows MJ, Riemann L. 2021. Quantifying nitrogen fixation by heterotrophic bacteria in sinking marine particles. Nat Commun 12:4085. https://doi.org/10.1038/ s41467-021-23875-6
- de Sousa Abreu R, Penalva LO, Marcotte EM, Vogel C. 2009. Global signatures of protein and mRNA expression levels. Mol Biosyst 5:1512– 1526. https://doi.org/10.1039/b908315d
- Vogel C, Marcotte EM. 2012. Insights into the regulation of protein abundance from proteomic and transcriptomic analyses. Nat Rev Genet 13:227–232. https://doi.org/10.1038/nrg3185
- Rocca JD, Hall EK, Lennon JT, Evans SE, Waldrop MP, Cotner JB, Nemergut DR, Graham EB, Wallenstein MD. 2015. Relationships between protein-encoding gene abundance and corresponding process are commonly assumed yet rarely observed. ISME J 9:1693–1699. https:// doi.org/10.1038/ismej.2014.252
- Jia M, Winkler MKH, Volcke EIP. 2020. Elucidating the competition between heterotrophic denitrification and DNRA using the resourceratio theory. Environ Sci Technol 54:13953–13962. https://doi.org/10. 1021/acs.est.0c01776
- Ishii S, Ikeda S, Minamisawa K, Senoo K. 2011. Minireview nitrogen cycling in rice paddy environments: past achievements and future challenges. Microb Environ 26:282–292. https://doi.org/10.1264/jsme2. ME11293
- Murphy AE, Bulseco AN, Ackerman R, Vineis JH, Bowen JL. 2020. Sulphide addition favours respiratory ammonification (DNRA) over complete denitrification and alters the active microbial community in salt marsh sediments. Environ Microbiol 22:2124–2139. https://doi.org/ 10.1111/1462-2920.14969
- Marzocchi U, Thorup C, Dam AS, Schramm A, Risgaard-Petersen N. 2022. Dissimilatory nitrate reduction by a freshwater cable bacterium. ISME J 16:50–57. https://doi.org/10.1038/s41396-021-01048-z
- Gazitúa MC, Vik DR, Roux S, Gregory AC, Bolduc B, Widner B, Mulholland MR, Hallam SJ, Ulloa O, Sullivan MB. 2021. Potential virus-mediated

- nitrogen cycling in oxygen-depleted oceanic waters. ISME J 15:981–998. https://doi.org/10.1038/s41396-020-00825-6
- Rodríguez-Ramos JA, Borton MA, McGivern BB, Smith GJ, Solden LM, Shaffer M, Daly RA, Purvine SO, Nicora CD, Eder EK, Lipton M, Hoyt DW, Stegen JC, Wrighton KC. 2022. Genome-resolved metaproteomics decodes the microbial and viral contributions to coupled carbon and nitrogen cycling in river sediments. mSystems 7:e0051622. https://doi. org/10.1128/msystems.00516-22
- Bushnell B. 2014. BBMap: a fast, accurate, splice-aware aligner. https:// www.osti.gov/servlets/purl/1241166.
- 44. Peng Y, Leung HCM, Yiu SM, Chin FYL. 2012. IDBA-UD: a *de novo* assembler for single-cell and metagenomic sequencing data with highly uneven depth. Bioinformatics 28:1420–1428. https://doi.org/10.1093/bioinformatics/bts174
- Kang DD, Li F, Kirton E, Thomas A, Egan R, An H, Wang Z. 2019. MetaBAT
 an adaptive binning algorithm for robust and efficient genome reconstruction from metagenome assemblies. PeerJ 7:e7359. https://doi. org/10.7717/peerj.7359
- Parks DH, Imelfort M, Skennerton CT, Hugenholtz P, Tyson GW. 2015. CheckM: assessing the quality of microbial genomes recovered from isolates, single cells, and metagenomes. Genome Res 25:1043–1055. https://doi.org/10.1101/gr.186072.114
- Olm MR, Brown CT, Brooks B, Banfield JF. 2017. dRep: a tool for fast and accurate genomic comparisons that enables improved genome recovery from metagenomes through de-replication. ISME J 11:2864–2868. https://doi.org/10.1038/ismej.2017.126
- Chaumeil P-A, Mussig AJ, Hugenholtz P, Parks DH, Hancock J. 2020.
 GTDB-Tk: a toolkit to classify genomes with the genome taxonomy

- database. Bioinformatics 36:1925–1927. https://doi.org/10.1093/bioinformatics/btz848
- Shaffer M, Borton MA, McGivern BB, Zayed AA, La Rosa SL, Solden LM, Liu P, Narrowe AB, Rodríguez-Ramos J, Bolduc B, Gazitúa MC, Daly RA, Smith GJ, Vik DR, Pope PB, Sullivan MB, Roux S, Wrighton KC. 2020. DRAM for distilling microbial metabolism to automate the curation of microbiome function. Nucleic Acids Res 48:8883–8900. https://doi.org/ 10.1093/nar/gkaa621
- Langmead B, Salzberg SL. 2012. Fast gapped-read alignment with Bowtie 2. Nat Methods 9:357–359. https://doi.org/10.1038/nmeth.1923
- Bushnell B, Rood J, Singer E. 2017. BBMerge accurate paired shotgun read merging via overlap. PLOS ONE 12:e0185056. https://doi.org/10. 1371/journal.pone.0185056
- Liao Y, Smyth GK, Shi W. 2014. featureCounts: an efficient general purpose program for assigning sequence reads to genomic features. Bioinformatics 30:923–930. https://doi.org/10.1093/bioinformatics/ btt656
- Robinson MD, McCarthy DJ, Smyth GK. 2010. edgeR: a bioconductor package for differential expression analysis of digital gene expression data. Bioinformatics 26:139–140. https://doi.org/10.1093/bioinformatics/btp616
- 54. Mauri M, Elli T, Caviglia G, Uboldi G, Azzi M. 2017. RAWGraphs: a visualisation platform to create open outputs. Proceedings of the 12th Biannual Conference on Italian SIGCHI Chapter (CHItaly '17) 28:1–5. https://doi.org/10.1145/3125571.3125585